Published in final edited form as:
Neuroimage. 2012 May 1; 60(4): 2316–2322. doi:10.1016/j.neuroimage.2012.02.005.

Correlations between FDG PET glucose uptake-MRI gray matter volume scores and apolipoprotein E ε4 gene dose in cognitively normal adults: a cross-validation study using voxel-based multi-modal partial least squares

Kewei Chen, Ph.D.[1,2,8,*], **Napatkamon Ayutyanont, Ph.D.**[1,8,*], **Jessica B.S. Langbaum, Ph.D.**[1,8], **Adam S. Fleisher, M.D**[1,6,8], **Cole Reschke, B.S.**[1,8], **Wendy Lee, M.S.**[1,8], **Xiaofen Liu, M.S.**[1,8], **Gene E Alexander, Ph.D.**[3,4,8], **Dan Bandy, M.S.**[1,8], **Richard J. Caselli, M.D.**[5,8], and **Eric M. Reiman, M.D.**[1,4,7,8]

[1]Banner Alzheimer's Institute and Banner Good Samaritan PET Center, Phoenix, AZ

[2]School of Mathematics and Statistics Sciences, Arizona State University, Tempe, AZ

[3]Department of Psychology and Evelyn F. McKnight Brain Institute

[4]Department of Psychiatry, University of Arizona, Tucson, AZ

[5]Departments of Neurology, Mayo Clinic, Scottsdale, AZ

[6]Department of Neurosciences, University of California, San Diego

[7]Division of Neurogenomics, Translational Genomics Research Institute, Phoenix, AZ

[8]Arizona Alzheimer's Consortium, Phoenix, AZ

Abstract

We previously introduced a voxel-based, multi-modal application of the partial least square algorithm (MMPLS) to characterize the linkage between patterns in a person's complementary complex datasets without the need to correct for multiple regional comparisons. Here we used it to demonstrate a strong correlation between MMPLS scores to characterize the linkage between the covarying patterns of fluorodeoxyglucose positron emission tomography (FDG PET) measurements of regional glucose metabolism and magnetic resonance imaging (MRI) measurements of regional gray matter associated with apolipoprotein E (APOE) ε4 gene dose (i.e., three levels of genetic risk for late-onset Alzheimer's disease (AD)) in cognitively normal, late-middle-aged persons. Coregistered and spatially normalized FDG PET and MRI images from 70% of the subjects (27 ε4 homozygotes, 36 ε4 heterozygotes and 67 ε4 non-carriers) were used in a hypothesis-generating MMPLS analysis to characterize the covarying pattern of regional gray matter volume and cerebral glucose metabolism most strongly correlated with APOE-ε4 gene dose. Coregistered and spatially normalized FDG PET and MRI images from the remaining 30% of the subjects were used in a hypothesis-testing MMPLS analysis to generate FDG PET-MRI gray matter MMPLS scores blind to their APOE genotype and characterize their relationship to APOE-ε4 gene dose. The hypothesis-generating analysis revealed covarying regional gray matter

*These co-authors contributed equally to this research.

volume and cerebral glucose metabolism patterns that resembled those in traditional univariate analyses of AD and APOE-ε4 gene dose and PET-MRI scores that were strongly correlated with APOE-ε4 gene dose ($p<1\times10^{-16}$). The hypothesis-testing analysis results showed strong correlations between FDG PET-MRI gray matter scores and APOE-ε4 gene dose ($p=8.7\times10^{-4}$). Our findings support the possibility of using the MMPLS to analyze complementary datasets from the same person in the presymptomatic detection and tracking of AD.

INTRODUCTION

Patients with Alzheimer's disease (AD) have abnormally low [18F] fluorodeoxyglucose (FDG) positron emission tomography (PET) measurements of the cerebral metabolic rate for glucose (CMRgl) in the precuneus, posterior cingulate, parietotemporal, and frontal cortex (Alexander et al., 2002; Landau et al., 2009; Langbaum et al., 2009; Minoshima et al., 1994). In structural magnetic resonance imaging (MRI)measurements, AD patients have reduced volume in the entorhinal cortex (Du et al., 2004; Jessen et al., 2006; Killiany et al., 2002), medial temporal lobe (Barta et al., 1997; Convit et al., 1997; Jack, Jr. et al., 1998), hippocampus (Ball et al., 1985; Basso et al., 2006), and whole brain volume (Fox et al., 1996). Decreased CMRgl (Drzezga et al., 2003; Herholz et al., 2007) and smaller hippocampal volume (Desikan et al., 2009; Grundman et al., 2002) have also been reported in patients with mild cognitive impairment (MCI) who subsequently developed AD.

We have used FDG PET and volumetric MRI in an ongoing longitudinal study to detect and track changes in brain function and brain structure in cognitively normal, late-middle aged persons with two copies, one copy, and no copies of the apolipoprotein E (APOE-ε4) allele, a major susceptibility gene in persons with AD with onset of dementia after age 60, representing at three levels of genetic risk for late-onset Alzheimer's disease. Our group, and others, have previously shown that ε4 homozygote (HM) and heterozygote (HT) groups have reduced cerebral glucose metabolic rates compared to noncarriers (NC) in the same brain regions as patients with probable AD and higher rates of the cerebral glucose metabolic rate decline in these and other brain regions (Higuchi et al., 1997; Reiman et al., 1996; Reiman et al., 2001; Reiman et al., 2005; Rimajova et al., 2008). Additionally, we have shown tendencies for smaller hippocampal volumes (Reiman et al., 1998) and whole brain atrophy rates (Chen et al., 2007; Reiman et al., 1998) in ε4 carriers compare to non-carriers. Similar findings that have been reported in mild cognitive impairment (MCI) and AD patients who are ε4 carriers(Drzezga et al., 2009; Filippini et al., 2009; Fleisher et al., 2005; Geroldi et al., 2000; Hashimoto et al., 2001; Liu et al., 2010; Pievani et al., 2011).

We previously developed a method, multi-modal partial least square (MMPLS), to capitalize on complementary information for two or more complex data sets (e.g., FDG PET CMRgl images of volumetric MRI gray matter maps (Chen et al., 2009)). The resulting spatial patterns were similar to those reported in conventional voxel-based univariate statistical analyses. The MMPLS derived global index of FDG PET CMRgl-MRI gray matter scores, distinguished healthy young and older subjects with significantly increased power compared to using either data alone.

In this study, we used the MMPLS and a cross-validation scheme to demonstrate a strong correlation between FDG PET-MRI gray matter MMPLS scores and APOE-ε4 gene dose, reflecting three levels of genetic risk for late-onset AD, in cognitively normal, late-middle-aged persons. To examine the increased strength of such correlation, we also estimated the correlation of APOE ε4 gene dose with FDG PET score alone or with MRI gray matter alone using unimodal PLS (Chen et al., 2008; McIntosh et al., 1996). The PET-MRI MMPLS scores and their linked covarying patterns were initially generated in a training data

set and then confirmed in a test set. Another extension to the previous method is the application of a permutation test to assess type-I error of the generated covarying patterns.

MATERIALS AND METHODS

Subjects and data

Cognitively normal volunteers 47 to 68 years of age were enrolled into a longitudinal cohort study (Caselli et al., 2001; Reiman et al., 1996; Reiman et al., 2005). Participants provided informed consent, agreeing not to be given any information about their APOE genotype and were studied under guidelines approved by the human subjects committees at Banner Good Samaritan Medical Center and the Mayo Clinic. Venous blood samples were drawn, and APOE genotypes were characterized with analysis by restriction fragment-length polymorphisms (Hixson and Vernier, 1990). Study participants were stratified into three groups: APOE ε4 HM, HT, and NC. Individuals who were enrolled reported a first-degree family history of probable Alzheimer's disease, and denied any cognitive symptoms. Additional inclusion criteria for participation consisted of a Folstein Mini-Mental State Examination (MMSE) score of at least 28, a Hamilton Depression Rating Scale (HAM-D) score less than 10, the absence of a current psychiatric disorder based on a structured psychiatric interview (Spitzer et al., 1990), and a normal neurological exam. Participants with a reported history of coronary artery disease, diabetes, or cerebrovascular accidents were excluded. Participants with clinically significant abnormalities, including but not limited to the presence of lacunar infarcts on their T1- weighted MRI, were also excluded. Note that, at the time these subjects' MRI were acquired, a complete clinical MRI exam, including T2-weighted images, was not acquired, hence evaluating more subtle evidence of cerebrovascular disease was not possible. During the baseline and at each follow-up visit (approximately every 2 years), a total of 250 cognitively normal subjects, including 54 APOE ε4 HM, 71 ε4 HT, and 125 ε4 NC, who were individually matched for their gender, age (within 3 years), and educational level (within 2 years) underwent a medical history and neurological examination, a structured psychiatric interview, the MMSE, the HAM-D, a battery of neuropsychological tests, FDG PET, and volumetric MRI.

Due to availability of the data at the time this analysis was conducted, only 130 cognitively normal subjects enrolled in this study, including 27 APOE ε4 HM, 36 ε4 HT, and 67 ε4 NC whose baseline FDG PET and volumetric MRI were acquired from the same PET/MRI scanner was included into this analysis. The three subject groups were matched in terms of their gender, age, and educational level. Note that since only a subset of subjects was included in this analysis, we were only able to match the subjects' characteristics in the group-level, rather than in the individual level as in the overall study.

Imaging data acquisition

Volumetric T1-weighted MRI and FDG PET were performed as previously described in (Chen et al., 2009; Reiman et al., 1996; Reiman et al., 1998; Reiman et al., 2004; Reiman et al., 2005). FDG PET was performed with a 951/31 ECAT scanner (Siemens, Knoxville, Tennessee), a 20-minute transmission scan, the intravenous injection of the 10 mCi of 18F-fluorodexoxyglucose, and a 60-minute dynamic sequence of emission scans as the subjects, who had fasted for at least 4 hours, lay quietly in the darkened room with their eyes closed and directed forward.

PET images were reconstructed using the filtered back projection with Hanning filter of 0.40 cycles per pixel and measured attenuation correction, resulting in 31 slices with in-plane resolution of about 8.5 mm, full width at half maximum (FWHM), an axial resolution of 5.0–7.1 mm FWHM, a 3.375 slice thickness and a 10.4 cm axial field of view.

MRI was performed using a 1.5 T Signa system (General Electric, Milwaukee, WI) and a T1-weighted, three-dimensional pulse sequence (radio-frequency-spoiled gradient recall acquisition in the steady state [SPGR], repetition time=33 ms, echo time=5 ms, α=30°, number of excitations=1, field of view=24 cm, imaging matrix=256 by 192, slice thickness=1.5 mm, scan time=13:36 min). The MRI data set consisted of 124 contiguous horizontal slices with in-plane voxel dimension of 0.94 by 1.25 mm.

Data-preprocessing

SPM5 (http://www.fil.ion.ucl.ac.uk/spm/) voxel based morphometry (VBM) was used to pre-process MRI data. Automated segmentation and normalization procedures were applied to each subject's MRI to exclude non-brain tissue and to generate maps of smoothed gray matter in the Montreal Neurological Institute (MNI) template coordinate space. A common mask was created and applied to the segmented gray matter maps to include gray matter voxels with an intensity value of at least 0.2, in every participant, for subsequent analyses.

Automated algorithms were also applied to each subject's PET image, co-registering to the same subject's MRI and deforming into MNI template space using the normalization parameters derived using the MRI segmentation and normalization procedures noted above. The PET images were then resampled to the same slice, matrix, and voxel size and number. Finally PET and MRI images were each smoothed to final 15 mm FWHM.

MMPLS analysis for hypothesis generation and testing

As described previously (Chen et al., 2009), to create X_{MRI} and X_{PET} numerical matrices for the MMPLS analysis, respective MRI or PET voxels within the brain mask were labeled as voxel 1, voxel 2, …, voxel P_X (where P_X is the number of voxels within the brain mask). At each given voxel location, a column vector of length n, where n is the number of subjects, was formed, such that element i is the voxel intensity for subject i (i=1,…,n).

Our informed MMPLS uses the combined matrix [X_{PET} X_{MRI}] as the independent block, unlike unimodal PLS which would use either X_{PET} or X_{MRI} for PET or MRI analysis. To incorporate information about subjects' APOE4 gene dose group membership, the dependent block in this MMPLS analysis designated APOE-ε4 non-carriers as 0, heterozygotes as 1 and homozygotes as 2.

Informed MMPLS uncovers the maximal covariance between a series of latent variables from the independent block and the dependent variable. The first latent variable, for example, is constructed as a linear combination of all variables in the independent block. Beginning with the original, X, the first latent variable of X is $t=Xw$ where $w=(w1, w2, \ldots)^T$ where w_j is a scalar for random variable x_j which is the jth column of X with norm $||w||=1$. The covariance of this latent variable and y $cov(t,y)=w'X'y$. The maximal covariance value, with respect to w, can be proven to be the square root of the largest eigenvalue of the matrix $\Omega=[X'YY'X]$ with w being the corresponding eigenvector of Ω. The second latent variable pair can be constructed in a similar way after the contributions of the first latent variable are regressed out (deflated) (Hoegaerts et al., 2003). The same procedure is then repeated to construct each subsequent latent variable pair, up to the L, where $L=rank(X)$. Note that MMPLS method is a global index thus is free from multiple comparisons issue.

To cross-validate the APOE-ε4 association with the spatial covarying pattern characterized by MMPLS, the data from each APOE-ε4 gene dose group was randomly partitioned into two groups. 70% of the total number of subjects was assigned to the training dataset for hypothesis generating and the remaining 30% to the testing dataset for hypothesis testing.

During the hypothesis generating MMPLS analysis, the FDG PET-MRI spatial covarying pattern was generated using the training dataset. The resulting covarying pattern was then applied to the testing dataset to generate the MMPLS score for each subject. For hypothesis testing of the MMPLS covarying pattern, the subject scores were then regressed against the number of APOE-ε4 alleles for subjects in the testing dataset. Informed MMPLS, with the APOE-ε4 gene dose as the predicted variable and the paired FDG PET and segmented gray matter volumes derived from MRI as the predictors, was applied to the pooled training datasets from NC, HT and HM groups to generate the covarying patterns.

This cross-validation is important for controlling the type-I error, since the MMPLS procedure is "informed" in that it maximizes the covariance between the predicted variable (APOE-ε4 gene dose) and the predictor datasets (FDG PET and structural MRI). With the cross validation, such dosage effects are independent of the MMPLS procedure maximizing the covariance between the predicted variable and the predictor datasets.

Using the similar hypothesis generating/testing procedure described above, we computed the uni-modal PLS-based APOE ε4 correlation coefficients with FDG PET subject scores or with MRI-gray matter subject scores for the subjects in the testing datasets. The PLS procedure is essentially the same except the independent block is either X_{PET} or X_{MRI} alone.

Assessing type-I error of the MMPLS covarying pattern

In addition to cross-validation for which there is no need to separately address type-I error for the APOE-ε4 dose effect over the testing dataset, a permutation test was conducted over the training dataset. This assessed the type-I error of the detected MMPLS patterns both in FDG PET and in volumetric MRI, and the obtained correlation of APOE-ε4 gene dose with the resulting MMPLS subject scores. For each of the 5000 random permutations, the informed MMPLS was run in the same manner as described above but for the randomly permutated APOE-ε4 gene dose and the non-permutated FDG PET and MRI data. Let r_0 be the correlation coefficient and V_0 the percentage overlap of the AD hypometabolic regions (Alexander et al., 2002) with the MMPLS-characterized FDG PET covarying pattern observed in the non-permuted MMPLS run, the 5000 permutations assessed the probability (type-I error) of obtaining a correlation coefficient $\geq r_0$ and the corresponding MMPLS AD FDG PET region overlap$\geq V_0$.

RESULTS

There were no significant differences among the three APOE-ε4 dosage groups in terms of age, gender ratio, education levels and neuropsychological scores (Table 1). Also the training and testing sets were not different in their APOE4 APOE-ε4 dosage ratio, age, gender ratio, educational levels and neuropsychological scores ($p>0.05$). In neurological orientation, Figure 1 shows the paired spatial covarying patterns for FDG PET and the segmented MRI gray matter volume separately. APOE-ε4 gene dose was associated with lower CMRgl in posterior cingulate, temporal, parietal and prefrontal cortex($p<0.05$). Similarly, increasing APOE-ε4 gene dose was associated with lower gray matter volume in parietal, anterior cingulate, temporal, hippocampus, parahippocampus and inferior frontal regions ($p<0.05$). To provide additional evidence that the observed gene dose effect on the MMPLS-characterized covarying patterns were not an artifact of the combination of measurements from a large number of voxels across multiple datasets, we conducted the random permutation test. Over the 5000 random permutations performed, there was none that had APOE-ε4/PET-MRI correlation coefficient $\geq r_0$ AND the overlap $\geq V_0$. In the other words, the estimated type-I error was lower than 1/5000 ($p<0.0002$). Qualitatively, we notice that significant correlations between the lowered CMRgl and lowered gray matter volume were limited to the vicinity of AD affected regions, and significant correlation

between APOE-ε4 gene dose and higher CMRgl or higher gray matter volume were not observed in any of area known to be associated with AD (at p=0.05 threshold).

Increasing APOE-ε4 gene dose was significantly correlated with higher PET-MRI MMPLS scores for individuals from both the training subject group (r=0.76, $p=1.1\times10^{-16}$) and the independent testing subject group (r=0.49, p=0.00087) as shown in Figure 2. This suggests that the observed correlation between PET-MRI MMPLS scores and APOE-ε4 gene dose was replicable and not an artifact of MMPLS procedure, maximizing the covariance between the APOE-ε4 dosage, FDG PET and volumetric MRI.

When only the FDG PET or MRI gray matter data was used alone in unimodal PLS, the independent testing dataset showed correlation of APOE4 dosage with FDG PET alone as r=0.34 (p=0.01085) or the one with MRI alone as r=0.22 (p=0.097).

DISCUSSION

This study illustrates the potential to capitalize on two or more complementary brain images from the same person using our voxel-based MMPLS to help in the presymptomatic detection and tracking of AD. In this study, we initially used the MMPLS to characterize the linkage between FDG PET and MRI gray matter patterns most closely associated with three levels of genetic risk for AD (i.e., the number of ε4 alleles in a person's APOE genotype) in cognitively normal late-middle-aged people. We confirmed this linkage in an independent data set; and we introduced a new cross-validation scheme to demonstrate that the significance levels generated using the MMPS were not inflated by the combination of measurements from a large number of voxels across the two datasets.

The paired covarying patterns for FDG PET CMRgl hypometabolism and the reduced MRI gray matter volume from hypothesis-generating MMPLS analysis resembled the patterns of CMRgl declines (Alexander et al., 2002; Landau et al., 2009; Langbaum et al., 2009; Minoshima et al., 1994) and structural changes observed separately in conventional univariate analyses of AD (Ball et al., 1985; Barta et al., 1997; Basso et al., 2006; Convit et al., 1997; Jack, Jr. et al., 1998) in regions previously implicated in patients with Alzheimer's dementia and APOE-ε4 gene (Chen et al., 2007; Reiman et al., 1996; Reiman et al., 1998; Reiman et al., 2001; Reiman et al., 2005; Reiman, 2005). FDG PET CMRgl hypometabolism was observed in the brain regions known to be preferentially affected in patients with AD, more specifically, in posterior cingulate, temporal, parietal and prefrontal cortex regions. The lower MRI gray matter volume was also observed in the vicinity of AD affected regions in parietal, anterior cingulate, temporal, hippocampus, parahippocampus and inferior frontal regions. Further substantiating the relevance of these findings to the pathology of AD, significant correlations between the lower CMRgl and lower gray matter volume were limited to the vicinity of AD affected regions, and significant correlation between APOE-ε4 gene dose and higher CMRgl or higher gray matter volume were not observed in any of area known to be associated with AD. This confirms the results from previous studies (Chen et al., 2007; Reiman et al., 1996; Reiman et al., 1998; Reiman et al., 2001; Reiman et al., 2005; Reiman, 2005) that, before the clinical AD onset, the APOE-ε4 carriers exhibit more CMRgl reduction and structural brain atrophy than NC and the extent of the CMRgl reduction and structural atrophy is correlated with the APOE-ε4 dosage. Such consistency also help validated the use of MMPLS to characterize the pattern of CMRgl and gray matter volume simultaneously.

While the regions associated with reduced CMRgl and gray matter are likely to reflect the changes in preclinical AD severity, the biological basis of the increases remains to be clarified. For instance, the regional CMRgl increases could reflect regional sparing

(following normalization for individual variations in whole brain metabolism), and some of the CMRgl and gray matter increases could reflect compensatory increases in neuronal activity and synaptic density.

As expected, the hypothesis testing analysis revealed that progressively increased risk of AD was associated with progressively increased FDG PET-MRI gray matter MMPLS subject scores derived from applying the covarying patterns generated in the hypothesis-generating MMPLS analysis. Such correlation was observed in both testing and training dataset suggesting that the strong correlation was replicable and not an artifact of the MMPLS procedure. The permutation test resulting in type-I error less than 0.0002 further confirmed that the observed correlation are not the results of an artifact of the combination of measurements from a large number of voxels across datasets. Note that this APOE-ε4 dosage effects was free of multiple comparisons, since it was global in nature.

This cohort of cognitively normal individuals at varying risk for AD have not yet been proven to develop symptomatic disease, or even have known AD pathology. However, by APOE-ε4 gene dose as risk alone (note all of our subjects were with family history of AD, a limitation further discussed below) we can identify associated patterns of glucose hypometabolism and gray matter volume loss similar to that seen in clinical dementia of the Alzheimer's type. This suggests the relevance of the findings presented here as potential true biomarkers of early pre-symptomatic Alzheimer's disease. By demonstrating clear covarying relationships between neurodegeneration (gray matter volume loss) and functional loss (glucose hypometabolism), in patterns associated with symptomatic AD, this analysis exemplifies the combined use of such pre-clinical biomarkers of disease to increase certainty of underlying AD pathology consistent with the new National Institute of Aging/ Alzheimer's Association (NIA-AA) research criteria for pre-clinical AD (Sperling et al., 2011).Studies in MCI patients (Arnaiz et al., 2001; Chen et al., 2011; Chetelat et al., 2003; Drzezga et al., 2003; Jack, Jr. et al., 1999; Spulber et al., 2010; Vemuri et al., 2009) and in asymptomatic familial early-onset AD mutation carriers (Kennedy et al., 1995) suggest that the relationship between the reduction in CMRgl and gray matter volume in AD-related region and AD risk is not limited to the APOE-ε4 allele. Based on these studies, we propose that the FDG PET MRI MMPLS score, which is based on such reduction in CMRgl and gray matter volume, could provide a quantitative presymptomatic inter-modal neuroimaging surrogate marker to help evaluate the individual and aggregate effects of putative genetic and non-genetic modifiers of AD risk for unusually early detection and tracking of AD.

Although APOE ε4 gene dose was significantly correlated with FDG PET-MRI MMPLS score, there was considerable overlap among the three genetic groups in their individual measurements. As we have noted (Reiman et al., 1996), neither genetic testing for APOE genotype, FDG PET nor MRI is clinically indicated to predict a cognitively normal individual's risk of AD. This information does not yet determine with sufficient accuracy whether or when an individual might develop AD. The use of the MMPLS score to accurately predict whether and when the person will develop AD still needs to be further examined.

Compared analyzing FDG PET and MRI together using MMPLS to analyzing FDG PET or MRI alone with unimodal PLS, we found that 1) the increased sensitivity is observed when using FDG PET and MRI together as compared using each separately alone; 2) the least significant (indeed insignificant) result for the MRI alone is consistent with our previous findings from the same cognitively healthy APOE ε4 NC/HT/HM cohort that FDG PET based posterior cingulate functional hypometabolism appeared earlier than the MRI based structurally observable abnormality prior to the onset of the disease; 3) despite the more subtle insignificant structural changes, the increased sensitivity, when combining FDG PET

and MRI information together, is not simply additive but in a more multiplicative and nonlinear manner enhancing the statistical power much more beyond using each alone and 4) studies with larger sample sizes are needed to confirm the increased sensitivity when using FDG PET and MRI jointly than using each alone.

As we have begun to acquire PIB PET images in the subjects enrolled in our cohort, we are exploring the possibility of extending our findings to addition of complementary data sets from the same subjects as sufficient amount of data became available (Reiman et al., 2009).

We note that there are some limitations for our current analysis. The first limitation is that all subjects included reported a first degree family history of probable AD. This may reduce our power to detect brain changes associated with the risk of AD since all three subject groups are likely to be associated with a higher risk than the general population. The second limitation is that we did not use the global scaling instead of data-driven scaling in this analysis. Based on (Borghammer et al., 2009), the global scaling could introduce spurious results (i.e. underestimation of APOE ε4 effect in our study. Thus, our results might be on the conservative side with regards to the APOE ε4 effects.

As we have previously noted, it may be possible to use the MMPLS to track the progression of AD by linking the patterns of longitudinal changes in different data sets in persons at differential genetic risk for AD; to link the patterns from other kinds of brain images from the same person; to extend the MMPLS to the linkage among more than two imaging and/or non-imaging (e.g,. genetic) data sets, and to capitalize on complementary complex data sets to help address a range of scientific and clinical questions. Additional studies are needed to clarify the value of this approach to the scientific study, presymptomatic detection, tracking and diagnosis of AD, the evaluation of AD-modifying treatments, and other research questions inside and outside the field of AD.

Reference List

Alexander GE, Chen K, Pietrini P, Rapoport SI, Reiman EM. Longitudinal PET Evaluation of Cerebral Metabolic Decline in Dementia: A Potential Outcome Measure in Alzheimer's Disease Treatment Studies. Am J Psychiatry. 2002; 159:738–745. [PubMed: 11986126]

Arnaiz E, Jelic V, Almkvist O, Wahlund LO, Winblad B, Valind S, Nordberg A. Impaired cerebral glucose metabolism and cognitive functioning predict deterioration in mild cognitive impairment. Neuroreport. 2001; 12:851–855. [PubMed: 11277595]

Ball MJ, Fisman M, Hachinski V, Blume W, Fox A, Kral VA, Kirshen AJ, Fox H, Merskey H. A new definition of Alzheimer's disease: a hippocampal dementia. Lancet. 1985; 1:14–16. [PubMed: 2856948]

Barta PE, Powers RE, Aylward EH, Chase GA, Harris GJ, Rabins PV, Tune LE, Pearlson GD. Quantitative MRI volume changes in late onset schizophrenia and Alzheimer's disease compared to normal controls. Psychiatry Res. 1997; 68:65–75. [PubMed: 9104754]

Basso M, Yang J, Warren L, Macavoy MG, Varma P, Bronen RA, van Dyck CH. Volumetry of amygdala and hippocampus and memory performance in Alzheimer's disease. Psychiatry Res. 2006; 146:251–261. [PubMed: 16524704]

Borghammer P, Aanerud J, Gjedde A. Data-driven intensity normalization of PET group comparison studies is superior to global mean normalization. Neuroimage. 2009; 46:981–988. [PubMed: 19303935]

Caselli RJ, Osborne D, Reiman EM, Hentz JG, Barbieri CJ, Saunders AM, Hardy J, Graff-Radford NR, Hall GR, Alexander GE. Preclinical cognitive decline in late middle-aged asymptomatic apolipoprotein E-e4/4 homozygotes: a replication study. J Neurol Sci. 2001; 189:93–98. [PubMed: 11535238]

Chen K, Ayutyanont N, Langbaum JB, Fleisher AS, Reschke C, Lee W, Liu X, Bandy D, Alexander GE, Thompson PM, Shaw L, Trojanowski JQ, Jack CR Jr, Landau SM, Foster NL, Harvey DJ,

Weiner MW, Koeppe RA, Jagust WJ, Reiman EM. Characterizing Alzheimer's disease using a hypometabolic convergence index. Neuroimage. 2011; 56:52–60. [PubMed: 21276856]

Chen, K.; Reiman, E.; Huan, Z.; Caselli, RJ.; Bandy, D.; Ayutyanont, N.; Alexander, GE. Linking functional and structural brain images with multivariate network analyses: A novel application of the partial least square method. 2009.

Chen K, Reiman EM, Alexander GE, Caselli RJ, Gerkin R, Bandy D, Domb A, Osborne D, Fox N, Crum WR, Saunders AM, Hardy J. Correlations between apolipoprotein E epsilon4 gene dose and whole brain atrophy rates. Am J Psychiatry. 2007; 164:916–921. [PubMed: 17541051]

Chen, K.; Rowe, CC.; Reschke, C.; Ayutyanont, N.; Lee, W.; Tran, H.; Villemagne, VL.; O'Keefe, G.; Reiman, EM. Combining PIB and FDG PET data to distinguish AD patients from normal controls: a multi-modal partial least square approach. Society of Nuclear Medicine Annual Meeting; 2008.

Chetelat G, Desgranges B, De lSV, Viader F, Eustache F, Baron JC. Mild cognitive impairment: Can FDG PET predict who is to rapidly convert to Alzheimer's disease? Neurology. 2003; 60:1374–1377. [PubMed: 12707450]

Convit A, de Leon MJ, Tarshish C, De SS, Tsui W, Rusinek H, George A. Specific hippocampal volume reductions in individuals at risk for Alzheimer's disease. Neurobiol Aging. 1997; 18:131–138. [PubMed: 9258889]

Desikan RS, Cabral HJ, Hess CP, Dillon WP, Glastonbury CM, Weiner MW, Schmansky NJ, Greve DN, Salat DH, Buckner RL, Fischl B. Automated MRI measures identify individuals with mild cognitive impairment and Alzheimer's disease. Brain. 2009; 132:2048–2057. [PubMed: 19460794]

Drzezga A, Grimmer T, Henriksen G, Muhlau M, Perneczky R, Miederer I, Praus C, Sorg C, Wohlschlager A, Riemenschneider M, Wester HJ, Foerstl H, Schwaiger M, Kurz A. Effect of APOE genotype on amyloid plaque load and gray matter volume in Alzheimer disease. Neurology. 2009; 72:1487–1494. [PubMed: 19339712]

Drzezga A, Lautenschlager N, Siebner H, Riemenschneider M, Willoch F, Minoshima S, Schwaiger M, Kurz A. Cerebral metabolic changes accompanying conversion of mild cognitive impairment into Alzheimer's disease: a PET follow-up study. Eur J Nucl Med Mol Imaging. 2003; 30:1104–1113. [PubMed: 12764551]

Du AT, Schuff N, Kramer JH, Ganzer S, Zhu XP, Jagust WJ, Miller BL, Reed BR, Mungas D, Yaffe K, Chui HC, Weiner MW. Higher atrophy rate of entorhinal cortex than hippocampus in AD. Neurology. 2004; 62:422–427. [PubMed: 14872024]

Filippini N, Zarei M, Beckmann CF, Galluzzi S, Borsci G, Testa C, Bonetti M, Beltramello A, Ghidoni R, Benussi L, Binetti G, Frisoni GB. Regional atrophy of transcallosal prefrontal connections in cognitively normal APOE epsilon4 carriers. J Magn Reson Imaging. 2009; 29:1021–1026. [PubMed: 19388128]

Fleisher A, Grundman M, Jack CR Jr, Petersen RC, Taylor C, Kim HT, Schiller DH, Bagwell V, Sencakova D, Weiner MF, DeCarli C, Dekosky ST, van Dyck CH, Thal LJ. Sex, apolipoprotein E epsilon 4 status, and hippocampal volume in mild cognitive impairment. Arch Neurol. 2005; 62:953–957. [PubMed: 15956166]

Fox NC, Freeborough PA, Rossor MN. Visualisation and quantification of rates of atrophy in Alzheimer's disease. Lancet. 1996; 348:94–97. [PubMed: 8676724]

Geroldi C, Laakso MP, DeCarli C, Beltramello A, Bianchetti A, Soininen H, Trabucchi M, Frisoni GB. Apolipoprotein E genotype and hippocampal asymmetry in Alzheimer's disease: a volumetric MRI study. J Neurol Neurosurg Psychiatry. 2000; 68:93–96. [PubMed: 10601411]

Grundman M, Sencakova D, Jack CR Jr, Petersen RC, Kim HT, Schultz A, Weiner MF, DeCarli C, Dekosky ST, van DC, Thomas RG, Thal LJ. Brain MRI hippocampal volume and prediction of clinical status in a mild cognitive impairment trial. J Mol Neurosci. 2002; 19:23–27. [PubMed: 12212787]

Hashimoto M, Yasuda M, Tanimukai S, Matsui M, Hirono N, Kazui H, Mori E. Apolipoprotein E epsilon 4 and the pattern of regional brain atrophy in Alzheimer's disease. Neurology. 2001; 57:1461–1466. [PubMed: 11673590]

Herholz K, Carter SF, Jones M. Positron emission tomography imaging in dementia. Br J Radiol. 2007; 80(Spec No 2):S160–S167. [PubMed: 18445746]

Higuchi M, Arai H, Nakagawa T, Higuchi S, Muramatsu T, Matsushita S, Kosaka Y, Itoh M, Sasaki H. Regional cerebral glucose utilization is modulated by the dosage of apolipoprotein E type 4 allele and alpha1-antichymotrypsin type A allele in Alzheimer's disease. Neuroreport. 1997; 8:2639–2643. [PubMed: 9295092]

Hixson JE, Vernier DT. Restriction isotyping of human apolipoprotein E by gene amplification and cleavage with HhaI. J Lipid Res. 1990; 31:545–548. [PubMed: 2341813]

Hoegaerts L, Suykens JAK, Vandewalle J, De Moor B. Kernel PLS variants for regression. Citeseer. 2003:203–208.

Jack CR Jr, Petersen RC, Xu Y, O'Brien PC, Smith GE, Ivnik RJ, Tangalos EG, Kokmen E. Rate of medial temporal lobe atrophy in typical aging and Alzheimer's disease. Neurology. 1998; 51:993–999. [PubMed: 9781519]

Jack CR Jr, Petersen RC, Xu YC, O'Brien PC, Smith GE, Ivnik RJ, Boeve BF, Waring SC, Tangalos EG, Kokmen E. Prediction of AD with MRI-based hippocampal volume in mild cognitive impairment. Neurology. 1999; 52:1397–1403. [PubMed: 10227624]

Jessen F, Feyen L, Freymann K, Tepest R, Maier W, Heun R, Schild HH, Scheef L. Volume reduction of the entorhinal cortex in subjective memory impairment. Neurobiol Aging. 2006; 27:1751–1756. [PubMed: 16309795]

Kennedy AM, Frackowiak RS, Newman SK, Bloomfield PM, Seaward J, Roques P, Lewington G, Cunningham VJ, Rossor MN. Deficits in cerebral glucose metabolism demonstrated by positron emission tomography in individuals at risk of familial Alzheimer's disease. Neurosci Lett. 1995; 186:17–20. [PubMed: 7783942]

Killiany RJ, Hyman BT, Gomez-Isla T, Moss MB, Kikinis R, Jolesz F, Tanzi R, Jones K, Albert MS. MRI measures of entorhinal cortex vs hippocampus in preclinical AD. Neurology. 2002; 58:1188–1196. [PubMed: 11971085]

Landau SM, Harvey D, Madison CM, Koeppe RA, Reiman EM, Foster NL, Weiner MW, Jagust WJ. Associations between cognitive, functional, and FDG PET measures of decline in AD and MCI. Neurobiol Aging. 2009

Langbaum JB, Chen K, Lee W, Reschke C, Bandy D, Fleisher AS, Alexander GE, Foster NL, Weiner MW, Koeppe RA, Jagust WJ, Reiman EM. Categorical and correlational analyses of baseline fluorodeoxyglucose positron emission tomography images from the Alzheimer's Disease Neuroimaging Initiative (ADNI). Neuroimage. 2009; 45:1107–1116. [PubMed: 19349228]

Liu Y, Paajanen T, Westman E, Wahlund LO, Simmons A, Tunnard C, Sobow T, Proitsi P, Powell J, Mecocci P, Tsolaki M, Vellas B, Muehlboeck S, Evans A, Spenger C, Lovestone S, Soininen H. Effect of APOE epsilon4 allele on cortical thicknesses and volumes: the AddNeuroMed study. J Alzheimers Dis. 2010; 21:947–966. [PubMed: 20693633]

McIntosh AR, Bookstein FL, Haxby JV, Grady CL. Spatial pattern analysis of functional brain images using partial least squares. Neuroimage. 1996; 3:143–157. [PubMed: 9345485]

Minoshima S, Foster NL, Kuhl DE. Posterior cingulate cortex in Alzheimer's disease. Lancet. 1994; 344:895. [PubMed: 7916431]

Pievani M, Galluzzi S, Thompson PM, Rasser PE, Bonetti M, Frisoni GB. APOE4 is associated with greater atrophy of the hippocampal formation in Alzheimer's disease. Neuroimage. 2011; 55:909–919. [PubMed: 21224004]

Reiman EM. In this issue: genetics, cholesterol, and the risk of Alzheimer's disease. J Clin Psychiatry. 2005; 66:938–939. [PubMed: 16013912]

Reiman EM, Caselli RJ, Chen K, Alexander GE, Bandy D, Frost J. Declining brain activity in cognitively normal apolipoprotein E epsilon 4 heterozygotes: A foundation for using positron emission tomography to efficiently test treatments to prevent Alzheimer's disease. Proc Natl Acad Sci USA. 2001; 98:3334–3339. [PubMed: 11248079]

Reiman EM, Caselli RJ, Yun LS, Chen K, Bandy D, Minoshima S, Thibodeau SN, Osborne D. Preclinical evidence of Alzheimer's disease in persons homozygous for the epsilon 4 allele for apolipoprotein E. N Engl J Med. 1996; 334:752–758. [PubMed: 8592548]

Reiman EM, Chen K, Alexander GE, Caselli RJ, Bandy D, Osborne D, Saunders AM, Hardy J. Functional brain abnormalities in young adults at genetic risk for late-onset Alzheimer's dementia. Proc Natl Acad Sci USA. 2004; 101:284–289. [PubMed: 14688411]

Reiman EM, Chen K, Alexander GE, Caselli RJ, Bandy D, Osborne D, Saunders AM, Hardy J. Correlations between apolipoprotein E epsilon4 gene dose and brain-imaging measurements of regional hypometabolism. Proc Natl Acad Sci USA. 2005; 102:8299–8302. [PubMed: 15932949]

Reiman EM, Chen K, Liu X, Bandy D, Yu M, Lee W, Ayutyanont N, Keppler J, Reeder SA, Langbaum JB, Alexander GE, Klunk WE, Mathis CA, Price JC, Aizenstein HJ, Dekosky ST, Caselli RJ. Fibrillar amyloid-beta burden in cognitively normal people at 3 levels of genetic risk for Alzheimer's disease. Proc Natl Acad Sci USA. 2009; 106:6820–6825. [PubMed: 19346482]

Reiman EM, Uecker A, Caselli RJ, Lewis S, Bandy D, de Leon MJ, De SS, Convit A, Osborne D, Weaver A, Thibodeau SN. Hippocampal volumes in cognitively normal persons at genetic risk for Alzheimer's disease. Ann Neurol. 1998; 44:288–291. [PubMed: 9708558]

Rimajova M, Lenzo NP, Wu JS, Bates KA, Campbell A, Dhaliwal SS, McCarthy M, Rodrigues M, Paton A, Rowe C, Foster JK, Martins RN. Fluoro-2-deoxy-D-glucose (FDG)-PET in APOEepsilon4 carriers in the Australian population. J Alzheimers Dis. 2008; 13:137–146. [PubMed: 18376055]

Sperling RA, Aisen PS, Beckett LA, Bennett DA, Craft S, Fagan AM, Iwatsubo T, Jack CR Jr, Kaye J, Montine TJ, Park DC, Reiman EM, Rowe CC, Siemers E, Stern Y, Yaffe K, Carrillo MC, Thies B, Morrison-Bogorad M, Wagster MV, Phelps CH. Toward defining the preclinical stages of Alzheimer's disease: recommendations from the National Institute on Aging-Alzheimer's Association workgroups on diagnostic guidelines for Alzheimer's disease. Alzheimers Dement. 2011; 7:280–292. [PubMed: 21514248]

Spitzer, R.; Williams, J.; Gibbon, M.; First, M. User's Guide for the Structured Clinical Interview for DSM-III-R (SCID). American Psychiatric Publishing; Washington, DC: 1990.

Spulber G, Niskanen E, MacDonald S, Smilovici O, Chen K, Reiman EM, Jauhiainen AM, Hallikainen M, Tervo S, Wahlund LO, Vanninen R, Kivipelto M, Soininen H. Whole brain atrophy rate predicts progression from MCI to Alzheimer's disease. Neurobiol Aging. 2010; 31:1601–1605. [PubMed: 18829136]

Vemuri P, Wiste HJ, Weigand SD, Shaw LM, Trojanowski JQ, Weiner MW, Knopman DS, Petersen RC, Jack CR Jr. MRI and CSF biomarkers in normal, MCI, and AD subjects: predicting future clinical change. Neurology. 2009; 73:294–301. [PubMed: 19636049]

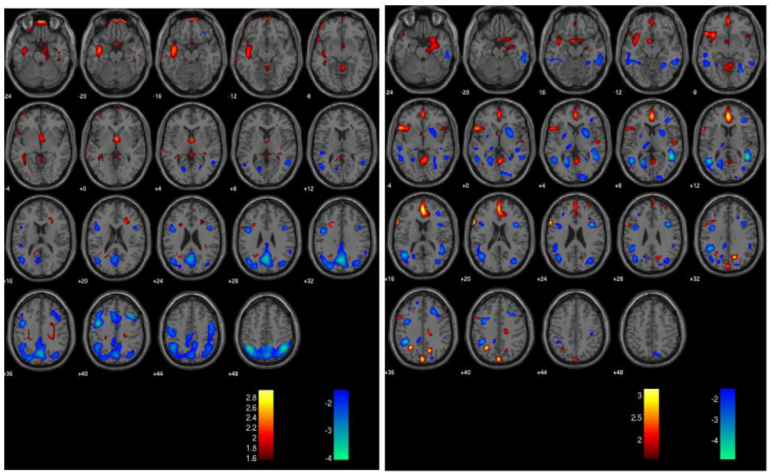

Figure 1.
The PET-MRI paired covarying patterns. Left: FDG PET with cool color showing negative CMRgl correlation with APOE-ε4 gene dose. Right: the segmented MRI gray matter volume with cool color showing negative gray matter volume in correlation with APOE-ε4 gene dose. The orientation of the images displayed is neurological (left of the image is the left hemisphere).

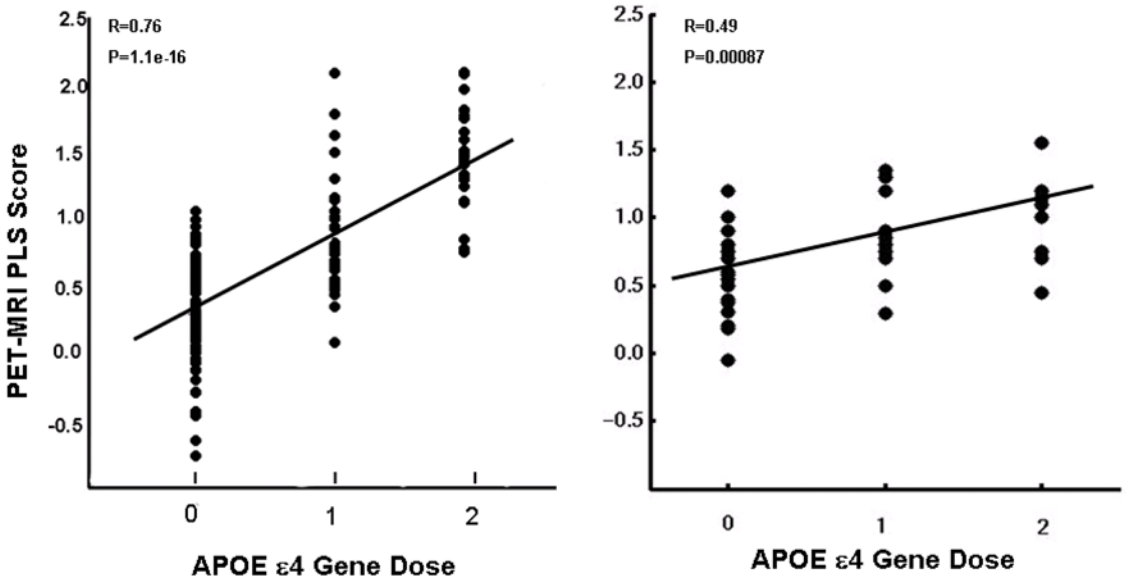

Figure 2.
Correlations between APOE4 gene dose and FDG PET-MRI MMPLS score. Left: training dataset, Right: testing dataset

Table 1

Subject characteristics, clinical ratings and neuropsychological scores

	ε4 noncarriers (n=67)	ε4 heterozygotes (n=27)	ε4 homozygotes (n=36)	*P*-value
Age	56.4±4.8	55.9±4.0	56.0±5.1	0.8
Years of education	15.8±1.6	15.4±1.5	15.1±3.2	0.3
Gender (F/M)	45/23	24/12	19/7	0.8
MMSE	29.7±0.5	29.8±0.5	29.9±0.6	0.5
AVLT				
Total learning	48.2±7.8	49.6±7.5	49.4±10.5	0.7
Short-term	9.6±2.5	10.2±2.4	9.9±3.4	0.6
Long-term	8.9±2.9	9.7±3.0	9.6±3.5	0.4

MMSE, Mini Mental State Exam; AVLT, Auditory verbal learning Test. Except gender ratio which was assessed using Chi-square test, other variables were examined using one-way ANOVA. Reported significances (P-values) are two-tailed.